

**In Silico Docking Analysis of Anti-malaria and Anti-typhoid Potentials of Phytochemical Constituents of Ethanol Extract of *Dryopteris dilatata***Chinyere B.C. Ikpa^{1*}, Ujupaul J.M. Ikezu¹, Maryjoy C. Maduwuba²¹Department of Chemistry Imo State University, Owerri, Imo state, Nigeria²Department of Microbiology Imo State University, Owerri, Imo State, Nigeria

ARTICLE INFO

Article history:

Received 05 March 2022

Revised 21 April 2022

Accepted 10 May 2022

Published online 04 June 2022

ABSTRACT

Traditional medicinal plants are a possible source of anti-malarial and anti-typhoid medications, and there is growing interest in the usage and development of herbal medicinal therapies for these ailments. The study aims to investigate the anti-malaria and anti-typhoid properties of *Dryopteris dilatata* leaves *in silico*. The plant leaves were extracted in ethanol and analyzed using Fourier transform infrared spectrometer (FTIR) and gas chromatography-mass spectrometry (GC-MS). The drug likeness and ADME predictions were done with OSIRIS property explorer and ADMETSAR webserver, while the molecular docking against dehydrogenase (Malaria target) and D-glutamate ligase enzyme (Typhoid Target) was done using Autodock Vina. The FT-IR results indicated the presence of -OH, CH₃, C-H aromatic and C=O functional groups while the GC-MS revealed thirteen (13) potential medicinal compounds, nine (9) compounds showed good pharmacokinetic properties having high human intestinal absorption, less toxic and good overall drug score. The molecular docking study revealed that three compounds, 1,2,3,4,7,8,9,10-Octahydro-12H-[1]benzothieno[2,3-d]pyrido[1,2-a]pyrimidin-12-one (-6.7 Kcal/mol), 4,7,9-Trihydroxy-2-methylnaphtho[2,3-b]furan-5,8-dione (-6.0 Kcal/mol), and 1,2,3-Triazol, 2-(E-4,4-dicyano-3-N-methylanilino-1,3-butadien-1-yl)-4-(methoxycarbonyl) (-6.3 Kcal/mol), gave better score for binding affinity than the control anti-malarial drug artesunate (-5.9 Kcal/mol). The typhoid docking also revealed the compounds, 4,7,9-trihydroxy-2-methylnaphtho[2,3-b]furan-5,8-dione (-8.6 Kcal/mol) and 1,2,3-Triazol, 2-(E-4,4-dicyano-3-N-methylanilino-1,3-butadien-1-yl)-4-(methoxycarbonyl)- (-8.3 Kcal/mol) had better binding affinity score than the reference anti-typhoid drug Ciprofloxacin (-8.1 Kcal/mol). The research justifies the local claims on the use of the plant and strengthens the relevance of these compounds as promising lead candidates for the treatment of Malaria and typhoid.

Copyright: © 2022 Ikpa *et al.* This is an open-access article distributed under the terms of the [Creative Commons Attribution License](https://creativecommons.org/licenses/by/4.0/), which permits unrestricted use, distribution, and reproduction in any medium, provided the original author and source are credited.

Keywords: *Dryopteris dilatata*, Dehydrogenase, Autodock, Pharmacokinetics, Typhoid, Malaria.

Introduction

Malaria is a preventable and curable disease, yet it remains an overwhelming tropical disease, with high infection and mortality rate.^{1,2} The protozoan parasite that causes malaria belongs to the genus *Plasmodium*.³ Malaria remains a major global public health problem despite the use of insecticide-treated bed nets, artemisinin-based combination treatments, and indoor residual spraying interventions,³ and the alarming spread of drug resistance,⁴ and limited number of effective drugs now available highlight the importance of discovering new anti-malarial compounds. Typhoid fever on the other hand is a bacterial infection caused by *Salmonella typhi*, especially in areas where access to clean water and other sanitation measures are limited. *Salmonella typhi* is a Gram-negative, motile, non-spore, non-capsulate bacilli which exist in nature primarily as parasites of the intestinal tract of man and other animals.⁵ Typhoid can manifest itself in a variety of ways, ranging from a severe septic infection to minor diarrhea and a moderate fever.

*Corresponding author. E mail: ikpacbc@gmail.com
Tel: +2348064305552

Citation: Ikpa CBC, Ikezu UJM, Maduwuba MC. *In Silico* Docking Analysis of Anti-malaria and Anti-typhoid Potentials of Phytochemical Constituents of Ethanol Extract of *Dryopteris dilatata*. Trop J Nat Prod Res. 2022; 6(5):772-782.

Official Journal of Natural Product Research Group, Faculty of Pharmacy, University of Benin, Benin City, Nigeria.

Fever, malaise, widespread stomach pain, and constipation are the most common symptoms. Untreated typhoid fever can cause delirium, obtundation, intestinal hemorrhage, bowel perforation, and death within a month of onset. Yearly, 21 million people acquire typhoid fever throughout the world it kills about 161,000 people each year and it has become increasingly resistant to antibiotics over time.⁶ Co-illnesses are highly common due to the geographical overlap of both infections. However, because both diseases share social circumstances that are critical to their transmission, the exact incidence of concurrent malaria and typhoid fever in most geographical areas is unknown. Individuals in areas where both diseases are endemic are at significant risk of contracting both diseases, either concurrently or as an initial illness superimposed on a secondary infection.⁷ Traditional medicinal plants are a possible source of anti-malarial and anti-typhoid medications, and there is growing interest in the usage and development of herbal medicinal therapies for these disorders. There are numerous plants that can be used as traditional medicine to treat various diseases. The therapeutic activities of plants are due to the presence of bioactive secondary metabolites in the crude plant material. One of such plant considered as having great medicinal importance is the fern *Dryopteris dilatata*. *Dryopteris dilatata* (broad buckler fern) also known as wood fern is a medicinal plant belonging to Dryopteridaceae family. It grows to 110 to 120 cm tall and 80 to 90 cm wide, with tripinnate dark green colour fronds, with the ribs covered in brown scales.⁸ It is known as Okpomie in Olomoro in Isoko South Local Government Area, Delta State, Nigeria and ukpakaiyi in Ehime Mbano Local Government Area of Imo State,

Nigeria. Oral interview with some Nigerians local herbalist explained that the plant is distributed in tropical regions of Nigeria and some Nigerians make concoctions of this plant for treatment of malaria, typhoid and diabetic conditions. The leaves and roots are the plant parts used for these purposes. Other common use of the plant is as anti-dandruff and worm-expeller. Different secondary metabolites including phenols, tannins, flavonoids, saponins, glycosides, steroids, terpenoids, and alkaloids have been reported from the extract of *D. dilatata* leaves.⁹

Limited scientific works exist that verifies the traditional claims of this plant. On Wistar rats, Akpotu *et al.*,¹⁰ reported *in-vitro* antioxidant activity of ethyl acetate and ethanol leaves extract. The ethanol extract of the leaves has been shown to have anti-diabetic and anti-hyperlipidemic properties¹¹. Akpotu *et al.*,¹² also reported the phytochemical and antioxidant characteristics of the plant's ethyl acetate leaf extract. The screening of therapeutic plants by spectrometric and chromatographic methods provides basic information on chemical and pharmacological activities, which helps to select the biologically active plants.¹³ In recent years, Fourier-transform infrared (FTIR) and gas chromatography-mass spectrometry (GC-MS) has been frequently employed for detection of functional groups and identification of various bioactive therapeutic compounds that are present in medicinal plants.^{14, 15, 16} Alcohols, alkaloids, nitro compounds, long chain hydrocarbons, organic acids, steroids, esters, and amino acids¹⁷ can all be detected using GC-MS, which only requires a tiny amount of plant extracts. As a result, the GC-MS technique was used in this work to detect and identify phytochemical components found in the medicinal plant, as there is no scientific work that verifies the traditional anti-malarial and anti-typhoid claims. The present study was aimed to investigate the compounds present in the ethanol extract of *Dryopteris dilatata* leaves using GC-MS and the anti-malaria and anti-typhoid potentials was predicted using Molecular docking.

Materials and Methods

Plant material collection

The leaves of *D. dilatata* were collected in March 2021 from Umuehie Umuezeala Nsu in Ehime Mbano LGA in Imo state, Nigeria. The plant was authenticated by Professor Mbagwu of the Plant Science and Biotechnology Department in Imo State University. A voucher herbarium specimen with collection data IMSUH-201 was deposited for future reference at the Imo State University Herbarium. The leaves were shade dried at room temperature and powdered with mortar and pestle kept in an amber colour container.²⁸

Preparation of the crude extract

The powdered plant material (1.3 kg) was soaked in 6.5 L of 80 percent ethanol (Carlo ERBA reagents SAS, France) for three days, and intermittently shaken at 130 rpm on an orbital shaker. The extract was filtered after 72 hours, and the residue was macerated twice in the same way. The filtrates were mixed together, concentrated using a rotary evaporator (Stuart, SO1, UK), and dried at 40°C in a Genlab oven.²⁸

Fourier transform infrared spectrometer (FTIR)

The FT-IR was performed with resolution in the spectral range of 4000–650 cm⁻¹ to detect the possible functional groups. 10 mg of the sample was encapsulated in 200 mg of KBr salt pellet, using a mortar and pestle, compressed into a thin pellet. The calibration was done by setting the Sample Scans at 30, Background Scans was set at 16 and Resolution was set to 8.²⁸

Gas chromatography-mass spectrometry (GC-MS) analysis

The sample was dissolved in ethanol and injected in an Agilent (Agilent 19091-433HP, USA) GC-MS coupled to a mass spectrophotometer MS (Agilent technologies) by author injection at the Multi-User Science Research Laboratory, Ahmadu Bello University, Zaria in Kaduna State, Nigeria. The following were the GCMS operating conditions for the analysis: Temperature in the oven: 50°C for 2 minutes, then 100°C at 10°C/min, then 200°C and held

isothermally for 10 minutes. The sample injection volume was 2µliters, and the carrier gas was helium at a rate of 1 mL per minute. The sample components were ionized at a voltage of 70 eV. The GC ran for a total of 24.50 minutes. The structures of the identified compounds were then compared to those in the NIST database using NIST14.Library (2018). The retention durations and mass spectra of the compounds were then compared to those of already known compounds in the NIST library (C:\Database\NIST14.L).²⁸

Drug likeness prediction

OSIRIS property explorer,¹⁸ was employed to determine likeness of drugs. Properties like Log S calculation, TPSA, log P calculation, molecular mass, and drug-likeness based on fragment and drug score of all the compounds have been established.

ADMET properties prediction

(ADMET) are acronyms for Absorption, Distribution, Metabolism, Excretion, and Toxicity. It contains a compound's (drug molecule's) pharmacokinetic profile and is important in evaluating its pharmacodynamic effects. Properties like bioavailability, brain penetration, oral absorption, carcinogenicity, and other human intestinal absorption properties of the active compounds have been determined using ADMETSAR webserver.¹⁹

Molecular docking

Ligand preparation

The identified compounds from GC-MS analysis that passed the Toxicity test were considered to study their assumed anti-malarial and anti-typhoid activities through docking studies. The structures of the compounds were obtained from Pubchem database²⁰ as sdf file, while that of the control drugs were obtained from Zinc15. All the downloaded compounds were converted into Mol, PDBQT and PDB file formats using OPEN BABEL software.²¹ The three-dimensional (3D) structures of compounds were optimized for docking conformation study. Hydrogen Bonds were added and the energy minimization was done using the CHARMM force field in PYRX software.

Protein target preparation

The 3D structure of the pFLDH complex and UDP-N-acetylmuramoyl-L-alanine: D-glutamate ligase enzyme were retrieved from Protein Databank with PDB IDs: 1LDG and 1E0D respectively. The 3D structures were prepared by removing water molecules, cofactor and substrate and the determination of the active sites was done using Pymol software. Further preparations including the addition of Kollman charges and polar hydrogen which were done using Autodock tools.

Docking studies

Screening of these compounds for protein ligand interactions was carried out using the AutodockVina²² in PYRX software. Based on several scoring functions, the software allows us to virtually screen a library of compounds and anticipate the strongest binders. The active site of pFLDH chosen was Ser 245, pro 246, ala 236, his 195, arg 171, leu 167, asp 168, ASN 140, arg 109 and the active site chosen for UDP-N-acetylmuramoyl-L-alanine: D-glutamate ligase enzyme was Gly111, Ser 112, Gly114, Lys115, Ser 116, Ser 117, Glu157, His183, Lys198, Asn268, Asn271, Arg302, and Asp317 (E. coli MurD numbering system). The docking was analyzed using the AutoDOCKVINA. Further docked result was visualized in Biovia discovery studio software.

Results and Discussion

Phytochemical screening

FT-IR and GC-MS analysis of ethanol extract of leaves *Dryopteris dilatata* was carried out, the results obtained were presented in Table 1 and Table 2 respectively. The compounds indicated in the FTIR analysis showed bands at 3381, 2922, 2855, 1736, 1457, and 1379 cm⁻¹ (Figure 1). The broad band at 3381 cm⁻¹ attributed to OH stretching in alcohol and phenol groups, 2922 and 2855 cm⁻¹ attributed to C-H

stretching vibration in alkanes group, Small band at 1736 cm^{-1} represents C=O stretching vibrations of carboxylic acid. 1457 , and 1379 cm^{-1} C-H stretching alkanes group. FT-IR analysis was used to identify the functional group of active components based on peak values in the region of infrared radiation. The GC-MS study (Figure 2) revealed the presence of the following compounds; 2-methyl-2-Hexene, 1H-Pyrrole-2,5-dione, 2-Pentanone, 4-hydroxy-4-methyl-, 1,3-Propanediamine, N-methyl-, Arsenous acid, tris(trimethylsilyl) ester, (3R,5aR,9S,9aS)-2,2,5a,9-Tetramethyloctahydro-2H-3,9a-methanobenzo[b]oxepine, 3,4-Altrosan, 2,4,6-Cycloheptatrien-1-one, 3,5-bis-trimethylsilyl-, Benzene, 1-[[4-(heptyloxy)phenyl]ethynyl]-4-propyl-, Piperonal-6-(4-methoxy-1-cyclohexen-1-yl)-, Benzothieno[2,3-d]pyrido[1,2-a]pyrimidin-12(12H)-one, 1,2,3,4,7,8,9,10-octahydro-, 4,7,9-Trihydroxy-2-methylnaphtho[2,3-b]furan-5,8-dione, 1,2,3-Triazol-2-(E-4,4-dicyano-3-N-methylanilino-1,3-butadien-1-yl)-4-(methoxycarbonyl)-. The compounds may be responsible agent for the medicinal properties of the plant.

Drug likeness prediction

The result of the OSIRIS Property Explorer²⁰ was presented in Table 3. Out of the identified compounds, four compounds (Arsenous acid, tris(trimethylsilyl) ester, 3,4-Altrosan, 2,4,6-Cycloheptatrien-1-one, 3,5-bis-trimethylsilyl- and Piperonal-6-(4-methoxy-1-cyclohexen-1-yl)-) failed the toxicity risks evaluation. Compounds with very low Clog P has high hydrophilicity and can be absorbed easily by the cell of proteins thus showing drug efficacy. The solubility score is measured by the least soluble (-6.5) to the most soluble (0.5). The total polar surface area (TPSA) tells the efficiency of the compounds in terms of membrane permeability. All the compounds had good TPSA scores.

ADMET prediction

ADMET (Absorption, Distribution, Metabolism, Excretion and Toxicity) properties were retrieved using admetSAR server. The result indicted two compounds (2-Methyl-2-hexene and Arsenous acid, tris(trimethylsilyl) ester) to be carcinogens. With the exclusion of 3,4-Altrosan that has very high mutagenic effect, all the identified compounds are having better human intestinal absorption score (Table

4). Higher human intestinal absorption (HIA) indicates that the compound of interest may be better consumed from the gastrointestinal tract upon oral administration. The penetration through the Blood-Brain Barrier (BBB) was also computed for all the compounds, All the compounds except (4,7,9-Trihydroxy-2-methylnaphtho[2,3-b]furan-5,8-dione) gave positive results to penetrate the BBB. In terms of predicting the efflux by P-glycoprotein from the cell, all the compounds except Piperonal, 6-(4-methoxy-1-cyclohexen-1-yl)- were non-inhibitors and while 3,4-Altrosan, 1,2,3-Triazol-2-(E-4,4-dicyano-3-N-methylanilino-1,3-butadien-1-yl)-4-(methoxycarbonyl)-, Piperonal-6-(4-methoxy-1-cyclohexen-1-yl)- and (3R,5aR,9S,9aS)-2,2,5a,9-Tetramethyloctahydro-2H-3,9a-methanobenzo[b]oxepine were substrates, the rest compounds were non-substrates. An inhibitor of P-glycoprotein means that drug will inhibit the efflux process from the cell and enhances the bioavailability and non-inhibitor of P-glycoprotein means that drug will efflux from the cell by P-glycoprotein and limits the bioavailability by pumping back into the lumen and may promote the elimination of that drug into the bile and urine.²³ A non-inhibitor of cytochrome P450 means that the molecule will not hinder the biotransformation of the compound (drug) metabolized by cytochrome P450.²⁴

Table 1: The major Functional groups of compounds present in the ethanol extract of *D. dilatata* leaves

Absorption peak	Functional group	Appearance
3381	OH	Broad medium peak
2922	Asymmetric Sp^3 C-H	Strong sharp
2855	Symmetric Sp^3 C-H	Strong sharp
1736	C=O	Strong sharp
1457,1379	Aromatic C-H	Medium

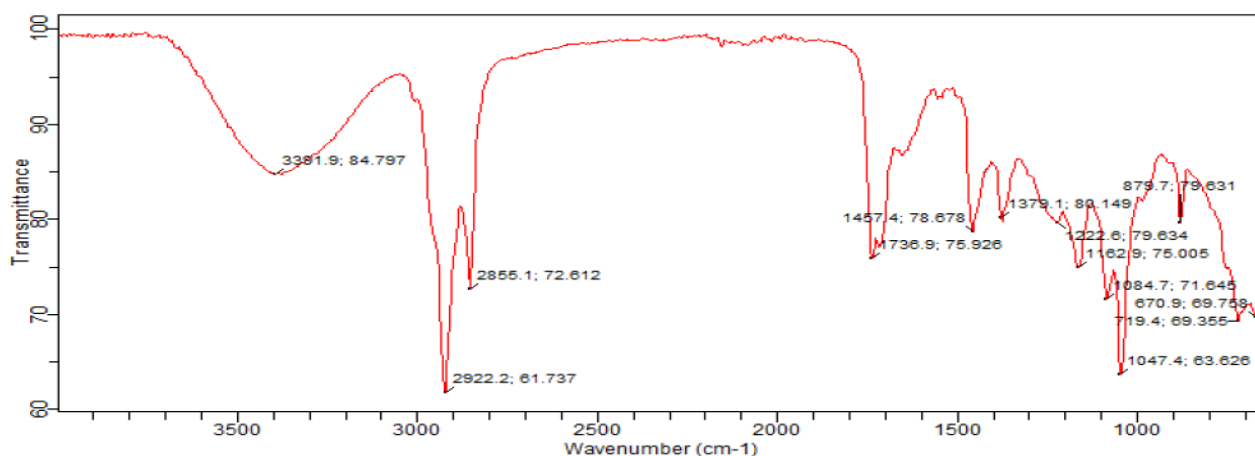


Figure 1: FTIR spectra of ethanol extract of *Dryopteris dilatata* leaves

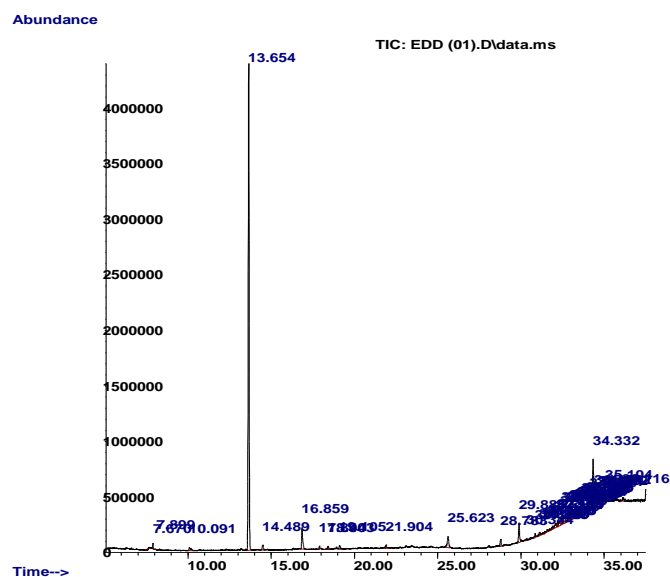


Figure 2: GC-MS spectra of ethanol extract of *Dyopteris dilatata* leaves

Table 2: The compounds detected in the ethanol extract of *D. dilatata* leaves using GC-MS

s/n	Compound	% comp	Molwt	Mol formula	Structure	Pub id
1	2-methyl-2-Hexene,	1.01	98.19	C ₇ H ₁₄		17656
2	1H-Pyrrole-2,5-dione	2.34	97.07	C ₄ H ₃ NO ₂		10935
3	2-Pentanone, 4-hydroxy-4-methyl-	50.93	116.16	C ₆ H ₁₂ O ₂		31256
4	1,3-Propanediamine, N-methyl-	2.16	88.15	C ₄ H ₁₂ N ₂		80511
5	Arsenous acid, tris(trimethylsilyl) ester	1.34	342.49	C ₉ H ₂₇ AsO ₃ Si ₃		180508
6	(3R,5aR,9S,9aS)-2,2,5a,9-Tetramethyloctahydro-2H-3,9a-methanobenzo[b]oxepine	2.24	222.37	C ₁₅ H ₂₆ O		521889
7	3,4-Altrosan	7.61	162.14	C ₆ H ₁₀ O ₅		548229

The Carcinogenic profile means that the carcinogenic compounds may undergo bioaccumulation in the human body and these compounds may lead to cancer in future if used for a long duration.

Molecular docking

The compounds that passed the toxicity test were further subjected to molecular docking. Docking was done to assess their anti-malarial and anti-typhoid potentials. The compounds and reference drugs were docked using the same algorithms and scoring functions. Artesunate and ciprofloxacin were the control drugs selected for anti-malarial and anti-typhoid study respectively.

Malaria docking

The PfLDH enzyme (figure 3a) was chosen for investigation because it controls energy production in plasmodium and has been considered a possible molecular target for anti-malarial medicines. Furthermore, this enzyme is detected in all five species that cause human malaria: *Plasmodium falciparum*, *Plasmodium vivax*, *Plasmodium ovale*, *Plasmodium malariae*, and *Plasmodium knowlesi*. PfLDH and human LDH have very similar biological roles, although their amino acid sequences are not. As a result, inhibiting this glycolytic enzyme in PfLDH selectively may not disrupt human LDH. The ligand binding site of Oxamate was chosen to be the active site of PfLDH. The result from this study showed that all the docked compounds bind either at the active site or very close to the site.²⁵

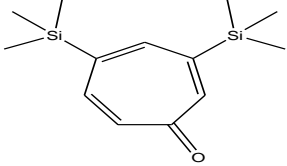
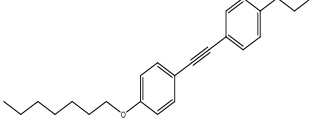
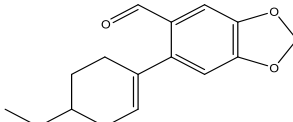
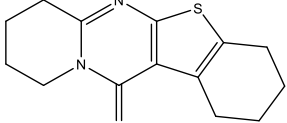
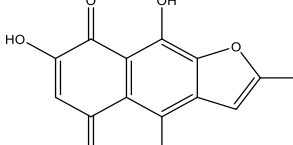
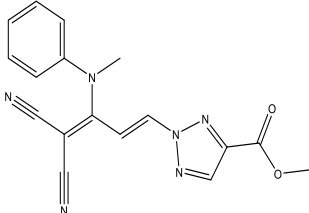
8	2,4,6-Cycloheptatrien-1-one, 3,5-bis-trimethylsilyl-	1.51	250.48	C ₁₃ H ₂₂ OSi ₂		610038
9	Benzene, 1-[[4-(heptyloxy)phenyl]ethynyl]-4-propyl-	1.77	334.5	C ₂₄ H ₃₀ O		610225
10	Piperonal-6-(4-methoxy-1-cyclohexen-1-yl)-	1.48	260.28	C ₁₅ H ₁₆ O ₄		621308
11	Benzothieno[2,3-d]pyrido[1,2-a]pyrimidin-12(12H)-one, 1,2,3,4,7,8,9,10-octahydro-	1.54	260.36	C ₁₄ H ₁₆ N ₂ OS		621369
12	4,7,9-Trihydroxy-2-methylnaphtho[2,3-b]furan-5,8-dione	1.09	260.20	C ₁₃ H ₈ O ₆		621370
13	1,2,3-Triazol-2-(E-4,4-dicyano-3-N-methylanilino-1,3-butadien-1-yl)-4-(methoxycarbonyl)-	1.05	334.33	C ₁₇ H ₁₄ N ₆ O ₂		5375845

Table 3: Toxicity and Drug likeness prediction using OSIRIS Property Explorer

S/n	Compound	Toxicity risks				C log P (≤5)	Solubility: log S (-6.5 to 0.5)	TPSA	Overall drug score
		Mutagenicity	Tumorigenic	Irritant	Reproductive effect				
1	2-Methyl-2-hexene	None	None	None	None	3.15	-1.96	0.00	0.45
2	1H-Pyrrole-2,5-dione	None	None	None	Medium	-1.01	-0.59	46.17	0.48
3	2-Pentanone, 4-hydroxy-4-methyl-	None	None	Medium	None	0.65	-1.16	37.3	0.3
4	1,3-Propanediamine, N-methyl-	None	None	None	None	-0.87	-0.31	36.05	0.64
5	Arsenous acid, tris(trimethylsilyl) ester	Medium	Medium	High	Medium	6.27	-6.54	27.69	0.05
6	(3R,5aR,9S,9aS)-2,2,5a,9-Tetramethyloctahydro-2H-3,9a-methanobenzo[b]oxepine	None	None	None	None	3.37	-3.6	9.23	0.41
7	3,4-Altrosan	High	None	None	None	-2.07	-0.23	82.45	0.4
8	2,4,6-Cycloheptatrien-1-one, 3,5-bis-trimethylsilyl-	None	None	High	None	4.62	-2.22	17.07	0.23

9	Benzene, 1-[[4-(heptyloxy)phenyl]ethynyl]-4-propyl-	None	None	None	None	7.67	-5.09	9.23	0.18
10	Piperonal-6-(4-methoxy-1-cyclohexen-1-yl)-	None	None	High	High	2.65	-3.64	44.76	0.15
11	Benzothieno[2,3-d]pyrido[1,2-a]pyrimidin-12(12H)-one, 1,2,3,4,7,8,9,10-octahydro-	None	None	None	None	2.8	-3.58	60.91	0.74
12	4,7,9-Trihydroxy-2-methylnaphtho[2,3-b]furan-5,8-dione	None	None	None	None	1.58	-3.89	107.9	0.49
13	1,2,3-Triazol-2-(E-4,4-dicyano-3-N-methylanilino-1,3-butadien-1-yl)-4-(methoxycarbonyl)-	None	None	None	Medium	1.66	-2.4	107.8	0.36

C log P (O/W): Logarithm of partition coefficient between n-octanol and water, log S: aqueous solubility, TPSA: Topological polar surface area

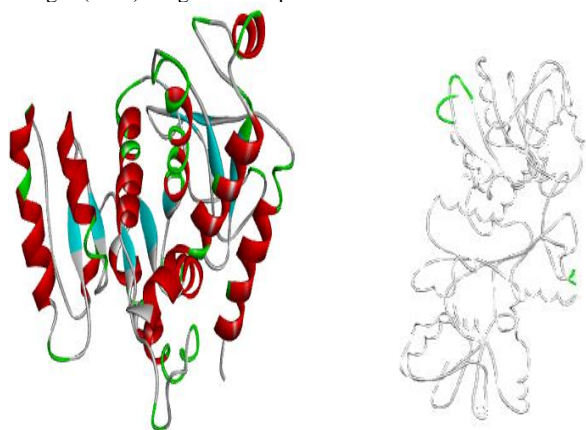


Figure 3: (a) PfLDH enzyme and (b) UDP-N-acetylmuramoyl-L-alanine:D-glutamate ligase enzyme respectively.

From the result, three compounds Benzothieno[2,3-d]pyrido[1,2-a]pyrimidin-12(12H)-one, 1,2,3,4,7,8,9,10-octahydro-(-6.7), 4,7,9-Trihydroxy-2-methylnaphtho[2,3-b]furan-5,8-dione (-6.0), and 1,2,3-Triazol, 2-(E-4,4-dicyano-3-N-methylanilino-1,3-butadien-1-yl)-4-(methoxycarbonyl) (-6.3) gave better score than the control anti-malarial drug artesunate (-5.9). The malaria docking results are presented in Table 5 and the 3D and 2D interactions are presented in Figures 4 and 5. Although, none of the residues of binding site was found to interact with artesunate neither in terms of hydrophobic nor hydrophilic interactions. However, artesunate was in close proximity of the binding cavity, and it had a good binding affinity scores it interacted with ALA-249 by forming a strong hydrogen bond, it further formed an alkyl bond with ILE-239. Figure 4a and 4b showed that Benzothieno[2,3-d]pyrido[1,2-a]pyrimidin-12(12H)-one, 1,2,3,4,7,8,9,10-octahydro- had the best binding affinity score (-6.7), it binds directly at the active site and it binds by making four *van der waals* interactions with the protease at SER-245, PRO-246, HIS-195, THR-139 and also made two alkyl bond interactions with VAL-138 and PRO-250.

Table 4: ADMET profile of the identified compounds predicted using ADMETSAR server

S/N	Compounds	HIA	BBB	CYP450 3A4	Carcinogenicity
		(value/probability)	(value/probability)	inhibitor/substrate	
1	2-Methyl-2-hexene	+0.9964	+0.9206	-/-	Carcinogens
2	1H-Pyrrole-2,5-dione	+0.9531	+ 0.9960	-/-	Non-carcinogens
3	2-Pentanone, 4-hydroxy-4-methyl-	+0.9954	+0.9806	-/-	Non-carcinogens
4	1,3-Propanediamine, N-methyl-	+0.9571	+0.8619	-/-	Non-carcinogens
5	Arsenous acid, tris(trimethylsilyl) ester	+0.7897	+0.9570	-/-	Carcinogens
6.	(3R,5aR,9S,9aS)-2,2,5a,9-Tetramethyloctahydro-2H-3,9a-methanobenzo[b]oxepine	+1.0000	+0.9852	-/+	Non-carcinogens
7	3,4-Altrosan	-0.8257	+0.6068	-/-	Non-carcinogens
8	2,4,6-Cycloheptatrien-1-one, 3,5-bis-trimethylsilyl-	+ 0.8486	+0.9442	-/+	Non-carcinogens
9	Benzene, 1-[[4-(heptyloxy)phenyl]ethynyl]-4-propyl-	+ 0.9869	+0.9731	-/+	Non-carcinogens

10	Piperonal, 6-(4-methoxy-1-cyclohexen-1-yl)-	+0.9792	+0.9422	+/+	Non-carcinogens
11	Benzothieno[2,3-d]pyrido[1,2-a]pyrimidin-12(12H)-one, 1,2,3,4,7,8,9,10-octahydro-	+0.9722	+0.9891	-/-	Non-carcinogens
12	4,7,9-Trihydroxy-2-methylnaphtho[2,3-b]furan-5,8-dione	+0.9874	-0.2782	-/-	Non-carcinogens
13	1,2,3-Triazol, 2-(E-4,4-dicyano-3-N-methylanilino-1,3-butadien-1-yl)-4-(methoxycarbonyl)-	+0.9465	+0.9803	-/+	Non-carcinogens

HIA: Human intestinal absorption, BBB: Blood Brain Barrier, CYP450: Cytochrome P450.

- ❖ - Means non inhibitor/ non substrate
- ❖ + means inhibitor/substrate

The second best score was shown by 1,2,3-Triazol, 2-(E-4,4-dicyano-3-N-methylanilino-1,3-butadien-1-yl)-4-(methoxycarbonyl)- (-6.3). It binds at the active site with one conventional H-bond with ASN-140, one carbon H-bond with LEU-163, one Pi-alkyl bond with MET-30 and Pi-Sigma bond with THR-101 respectively. However, 4,7,9-Trihydroxy-2-methylnaphtho[2,3-b]furan-5,8-dione, the compound with the third best score (-6.0) also bind firmly to the active site of the protease and it stabilized the active site through one conventional hydrogen bond SER-245, three Pi-alkyl bonds ALA-236, PRO-250, PRO-246 and a Pi-Pi T-shaped bond with the acid residue HIS-195.

Typhoid docking

Salmonella typhi is food-borne as well as water-borne pathogen, which is the main cause of typhoid fever. This disease is affecting people in both developing and underdeveloped countries. The emergence of multidrug resistance in *S. typhi* has encouraged researchers towards targeting novel pathways. UDP-N-acetylmuramoyl-L-alanine: D-glutamate ligase enzyme (figure 3b) is involved in cell wall synthesis of the bacterium. UDP-N-acetylmuramoyl-L-alanine: D-glutamate ligase is one of the vital enzyme that is crucial for the intracellular biosynthesis of peptidoglycan²⁶.

Table 5: Malaria docking result showing the types of interactions and the amino acids involved.

s/n	Compound	CID	BA (Kcal/mol)	Types of interaction	Amino acids involved
1	Artesunate	ZINC0000140	-5.9	- Conventional hydrogen bond - Alkyl	CHB: ALA249 ALK: ILE 239
2	1H-Pyrrole-2,5-dione	10935	-4.5	- Conventional hydrogen bond - van der Waals - Pi-Alkyl	CHB: SER245, ARG171 VDW: ALA236,LEU167 ,ARG109,HIS195,ILE31 ,THR101 Pi-ALK: PRO246, PRO250
3	2-Pentanone, 4-hydroxy-4-methyl-	31256	-4.6	- Conventional hydrogen bond - van der Waals - Unfavourable bumps - Unfavourable donor donor	CHB: HIS195,ASN140 VDW: LEU167,ARG171 ,ALA236,PRO246,SER245,TRP107,LEU163, VAL138,PRO245 UDD: ARG109
4	1,3-Propanediamine, N-methyl-	80511	-3.6	- Conventional hydrogen bond - Carbon hydrogen bond - van der Waals - Unfavourable bumps - Unfavourable donor donor	CHB: VAL138 VDW: ALA236, TRP107, PRO250, LEU107, HIS195,VAL142 UDD: ARG109,ASN140
5	(3R,5aR,9S,9aS)-2,2,5a,9-Tetramethyloctahydro-2H-3,9a-methanobenzo[b]oxepine	521889	-5.5	- van der Waal - Alkyl - Pi-Alkyl	VDW: SER170,ARG171 , ALA252,ALA248 ALK: TYR174 Pi-ALK: ALA249

6	Benzene, 1-[[4-(heptyloxy)phenyl]ethynyl]-4-propyl-	610225	-5.0	- van der Waal - Alkyl - Pi-Alkyl - Pi-Pi T-shaped	VDW: SER170, ARG171, PRO250 ALK: PRO184,ALA249, HIS243,PRO246,ILE239 Pi- ALK: VAL248,TYR247 PPT: TYR174
7	Benzothieno[2,3-d]pyrido[1,2-a]pyrimidin-12(12H)-one, 1,2,3,4,7,8,9,10-octahydro-	621369	-6.7	- van der Waal - Alkyl	VDW: SER245, PRO246, HIS195, THR139 ALK: VAL138, PRO250
8	4,7,9-Trihydroxy-2-methylnaphtho[2,3-b]furan-5,8-dione	621370	-6.0	- Conventional hydrogen bond - Pi-Alkyl - Pi-Pi T-shaped	CHB: SER245 Pi-ALK: ALA236, PRO250, PRO246 PPT: HIS195
9	1,2,3-Triazol, 2-(E-4,4-dicyano-3-N-methylanilino-1,3-butadien-1-yl)-4-(methoxycarbonyl)-	5375845	-6.3	- Conventional hydrogen bond - Carbon hydrogen bond - Pi-Alkyl - Pi-Sigma	CHB: ASN140 C-HB: LEU163 Pi-ALK: MET30 Pi-S: THR101

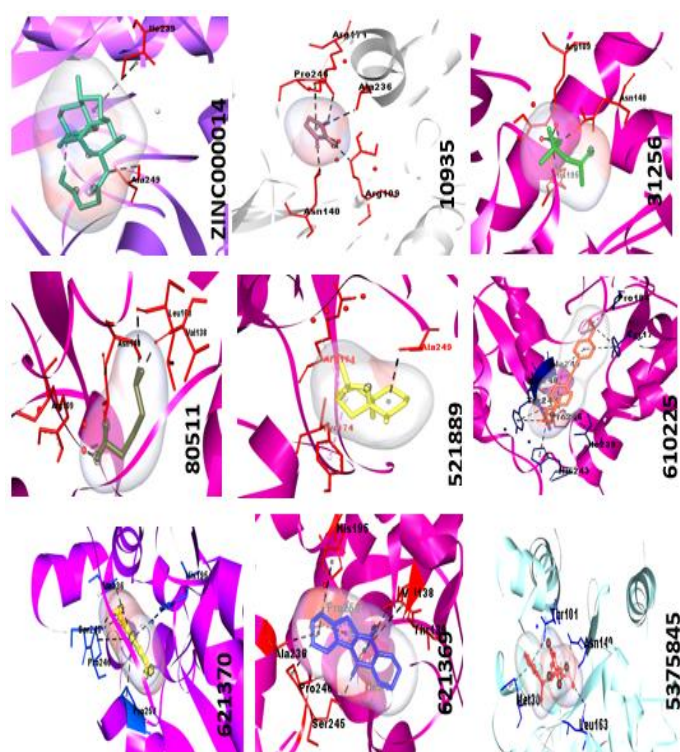


Figure 4: 3D representation of the Malaria docking results

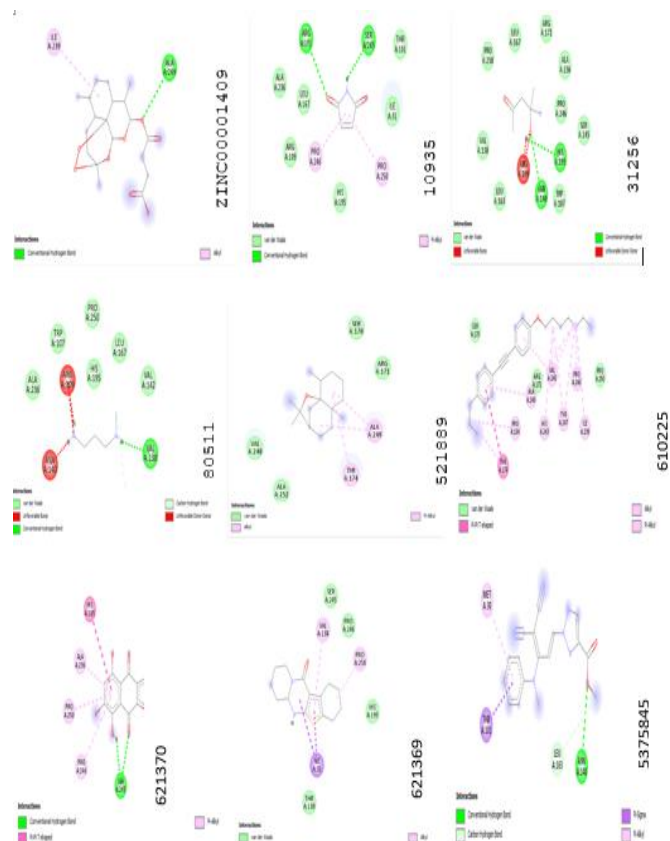


Figure 5: 2D representation of the Malaria docking result

5	(3R,5aR,9S,9aS)-2,2,5a,9-Tetramethyloctahydro-2H-3,9a-methanobenzo[b]oxepine	521889	-7.2	- van der Waals	VDW: ASN178, ASP214, ASP213, ASN211, VAL232, PHE230, THR270,HIS267, GLN266
6	Benzene, 1-[[4-(heptyloxy)phenyl]ethynyl]-4-propyl-	610225	-6.7	- Carbon Hydrogen bond - Alkyl - Pi-Alkyl	CHB: ASN268 ALK: ILE139, LYS319 Pi-ALK: ALA328
7	Benzothieno[2,3-d]pyrido[1,2-a]pyrimidin-12(12H)-one, 1,2,3,4,7,8,9,10-octahydro-	621369	-8.1	- Conventional hydrogen bond - Carbon hydrogen bond - van der Waal - Alkyl - Pi-Alkyl - Pi-Donor Hydrogen bond	CHB: SER116,LYS319 C-HB: GLY114 VDW: SER112 ALK: HIS267, ARG302 Pi-ALK: LYS319 PDHB: GLY114
8	4,7,9-Trihydroxy-2-methylnaphtho[2,3-b]furan-5,8-dione	621370	-8.6	- Conventional hydrogen bond - Pi-Cation - Pi-Anion - Pi-Alkyl - Pi-Pi T-shaped - Unfavourable Donor Donor	CHB: ASN268, ASP317, SER325 Pi-Cat: HIS267 Pi-An: ASP317 Pi-ALK: ARG302 PPT: ARG302 UDD: THR117
9	1,2,3-Triazol, 2-(E-4,4-dicyano-3-N-methylanilino-1,3-butadien-1-yl)-4-(methoxycarbonyl)-	5375845	-8.3	- Conventional hydrogen bond - Carbon hydrogen bond - van der Waal - Pi-Cation - Pi-Donor Hydrogen bond - Pi-Pi stacked - Pi-Alkyl - Amide-Pi stacked	CHB: THR117, SER116 C-HB: SER112, SER325 VDW: LYS115 Pi-Cat: HIS267 PDHB: SER112 PPS: GLY114 Pi-ALK: ARG302, ALA328 APS: GLY114

The monomer unit of peptide is assembled in the biosynthetic process of bacterial peptidoglycan by sequential accumulation of L-alanine, D-glutamic acid, meso-diamino-pimelic acid or lysine, and D-alanyl-D-alanine to UDP-N-acetylmuramic acid (UDP-MurNAc)2. A highly tailored ADP-forming ligase catalyzes each step of the peptide monomer addition procedure. The D-glutamate-adding enzyme, or UDP-MurNAc-L-alanine: D-glutamate ligase, catalyzes the addition of D-glutamate to UDP-MurNAc-L-Ala (UMA).²⁷ The synthetic process of peptidoglycan production can be shut down by blocking the D-glutamate ligase enzyme. The potential inhibitors of enzyme used in the study are the identified compounds and docking control drug (ciprofloxacin). The result from the molecular docking showed that the control drug and three other compounds can be potential inhibitors. The binding affinity score of the control drug Ciprofloxacin (-8.1) was good and it interacted with the protease through five strong hydrogen bonds, four conventional hydrogen bonds with ASN-268,ASN-271,ARG-302,THR-117and one C-hydrogen bond with SER116. Other interactions of ciprofloxacin were hydrophobic interactions with LYS-319 and HIS-267. The binding affinity energy and other information are presented in Table 6. When the binding affinity energy of control drug was compared with the compounds', it was observed that 4,7,9-Trihydroxy-2-methylnaphtho[2,3-b]furan-5,8-

dione had the highest negative binding affinity with (-8.6Kcal/mol) followed by 1,2,3-Triazol,2-(E-4,4-dicyano-3-N-methylanilino-1,3-butadien-1-yl)-4-(methoxycarbonyl)- with (-8.3Kcal/mol) and Benzothieno[2,3-d]pyrido[1,2-a]pyrimidin-12(12H)-one, 1,2,3,4,7,8,9,10-octahydro (-8.1 Kcal/mol) had the same binding affinity as the control drug. The three compounds bonded firmly to the active site of the protein. The 3D and 2D representations of the interactions are presented in Figures 6 and 7. The compound 4,7,9-Trihydroxy-2-methylnaphtho[2,3-b]furan-5,8-dione bonded to the active site through three conventional H-bonds with ASN-268, ASP-317, SER-325, also forming non-covalent interactions with HIS-267 and ASP-317. It further interacted covalently with amino acids ARG-302, ARG-302 and THR-117. Among the three compounds that exhibited potential inhibitors, the second compound; 1,2,3-Triazol,2-(E-4,4-dicyano-3-N-methylanilino-1,3-butadien-1-yl)-4-(methoxycarbonyl)- bonded to active site through hydrophilic and hydrophobic interactions, it interacted with the active site through four hydrogen interactions forming two conventional hydrogen bonds with THR-117, SER-116 and two C-hydrogen bond with SER-112, SER-325, other interactions were van der Waal and Pi-Cation interactions with HIS-267, Pi-Donor Hydrogen bond with SER-112, Pi-Pi stacked and Amide-Pi stacked interactions with GLY-114 and Pi-Alkyl with

ARG-302, ALA-328. The third compound Benzothieno[2,3-d]pyrido[1,2-a]pyrimidin-12(12H)-one, 1,2,3,4,7,8,9,10-octahydro bonded to the active site through hydrogen bond with SER-116, LYS-319 and GLY-114, *Van der waal* interaction with SER-112, Pi-Donor Hydrogen bond with GLY114 and through alkyl and Pi-alkyl with HIS-267, ARG-302 and LYS-319 respectively. This computational study could lead to the development of new anti-malarial and anti-typhoid medications with fewer side effects and a greater focus on the target. The long-term objective is to validate our *in-silico* findings through *in vitro* and *in vivo* research.

Conclusion

Herein, the research found out that the ethanol leaf extract of *D. dilatata* can be used for the prevention and treatment of malaria and typhoid fever. The results of this study suggest that extracts of *D. dilatata* represent a dependable source of novel bioactive compounds for pharmaceutical applications. Therefore, further research is encouraged which may include; the analysis of other chemical extracts of the plant, isolation of pure compounds from the plant and *in vivo* /*in vitro* evaluation study to further validate the computational findings.

Conflict of Interest

The authors declare no conflict of interest.

Authors' Declaration

The authors hereby declare that the work presented in this article are original and that any liability for claims relating to the content of this article will be borne by them.

Acknowledgements

We are grateful to Tertiary education trust fund (TETFUND) for providing the financial support for the procurement of chemicals, laboratory reagents and equipments, as well as transport expenses. Grant number TETFUND/IBR/PROJECT INTERVENTION/2015-2016 MERGED/BATCH 5/SN 08/IMSU Owerri.

References

- Julianna SD and Nawa MN. Malaria and Pregnancy: A Global Health Perspective. *Rev Obstet Gynecol.* 2009; 2(3):186-192.
- Laloo DG, Olukoya P, Oliario P. Malaria in adolescence: burden of disease, consequences, and opportunities for intervention. *The Lancet Infect Dis.* 2006; 6(12):780-793.
- Sato S. Plasmodium—a brief introduction to the parasites causing human malaria and their basic biology. *J Phys Anthr.* 2021; 40(1):1-3.
- Shibeshi MA, Kifle ZD, Atnafie SA. Antimalarial drug resistance and novel targets for antimalarial drug discovery. *Infect Drug Res.* 2020; 13:4047-4060.
- Ammah A, Nkuo-Akenji T, Ndip R, Deas JE. An update on concurrent malaria and typhoid fever in Cameroon. *Trans R Soc Trop Med Hyg.* 1999; 93(2):127-129.
- Crump JA and Mintz ED. Global trends in typhoid and paratyphoid fever. *Clin Infect Dis.* 2010; 50(2):241-246.
- Keong BC and Sulaiman W. Typhoid and malaria co-infection—an interesting finding in the investigation of a tropical fever. *The Malay J Med Sci.* 2006; 13(1):74.
- Rünk K, Zobel M, Zobel K. Biological Flora of the British Isles: *Dryopteris carthusiana*, *D. dilatata* and *D. expansa*. *J Ecol.* 2012; 100(4):1039-1063.
- Cao H, Chai TT, Wang X, Morais-Braga MF, Yang JH, Wong FC, Wang R, Yao H, Cao J, Cornara L, Burlando B. Phytochemicals from fern species: potential for medicine applications. *Phytochem Rev.* 2017; 16(3):379-440.
- Ajirioghene A, Ani C, Nworgu C, Pamela O, Uzoma I, Uzoigwe J, Mercy A, Ogochukwu N, Onwujekwe O. Antidiabetic and anti-hyperlipidemic effects of ethanolic extract of *Dryopteris dilatata* leaves. *J Diab Endocrinol.* 2018; 9(3):20-27.
- Ajirioghene AE, Ghasi SI, Ewhre LO, Adebayo OG, Asiwé JN. Anti-diabetogenic and *in vivo* antioxidant activity of ethanolic extract of *Dryopteris dilatata* in alloxan-induced male Wistar rats. *Biomarkers.* 2021; 26(8):718-725.
- Ajirioghene A, Celestine A, Toby A, Adaobi O, Francis A, Nnaemeka U, Patrick U, Chukwuka E, Jide U, Pamela A, Samuel G. Phytochemical and *in vitro* antioxidant properties of ethyl acetate leaf extract of *Dryopteris dilatata* on Wistar rats. *Afr J Biotechnol.* 2021; 20(8):318-324.
- Juszczak AM, Zovko-Končić M, Tomczyk M. Recent trends in the application of chromatographic techniques in the analysis of luteolin and its derivatives. *Biomol.* 2019; 9(11):731.
- Durazzo A, Lucarini M, Kiefer J, Mahesar SA. State-of-the-art infrared applications in drugs, dietary supplements, and nutraceuticals. *J Spec.* 2020; (2):2020.
- Njoku UO, Umeh CG, Ougofor MO. Phytochemical profiling and GC-MS analysis of aqueous methanol fraction of *Hibiscus asper* leaves. *FJ Pharm Sci.* 2021; 7(1):1-5.
- Hakani DS. Estimation of drug-likeness properties of GC-MS separated bioactive compounds in rare medicinal *Pleionemaculata* using molecular docking technique and SwissADME *in silico* tools. *NMA in Health Informatics and Bioinformatics.* 2021; 10(1):1-36.
- Razack S, Kumar KH, Nallamuthu I, Naika M, Khanum F. Antioxidant, Biomolecule Oxidation Protective Activities of *Nardostachys jatamansi* DC and Its Phytochemical Analysis by RP-HPLC and GC-MS. *Antioxidants (Basel).* 2015; 4(1):185-203.
- Srivastava R. Theoretical Studies on the Molecular Properties, Toxicity, and Biological Efficacy of 21 New Chemical Entities. *ACS omega.* 2021; 6(38):24891-24901.
- Norinder U and Bergström CA. Prediction of ADMET properties. *Chem Med Chem: Chem Enab Drug Discov.* 2006; 1(9):920-937.
- Kim S, Thiessen PA, Bolton EE, Chen J, Fu G, Gindulyte A, Han L, He J, He S, Shoemaker BA, Wang J. PubChem substance and compound databases. *Nucleic Acids Res.* 2016; 44 (D1):D1202-1213.
- O'Boyle NM, Banck M, James CA, Morley C, Vandermeersch T, Hutchison GR. Open Babel: An open chemical toolbox. *J Chem-Info.* 2011; 3(1):1-4.
- Trott O and Olson AJ. AutoDockVina: improving the speed and accuracy of docking with a new scoring function, efficient optimization, and multithreading. *J Comp Chem.* 2010; 31(2):455-461.
- Finch A and Pillans P. P-glycoprotein and its role in drug-drug interactions. *Aust Prescr.* 2014; 37(4):137-139.
- Cheng F, Li W, Zhou Y, Shen J, Wu Z, Liu G, Lee PW, Tang Y. AdmetSAR: A Comprehensive Source and Free Tool for Assessment of Chemical ADMET Properties. *J Chem Info Model.* 2012; 52(11):3099-3105.
- Blake J. Chemoinformatics – predicting the physicochemical properties of “drug-like” molecules. *Curr Opin Biotechnol.* 2000; 11(1):104-107.
- Škedelj V, Tomašić T, Lucija PM, Zega A. ATP-Binding Site of Bacterial Enzymes as a Target for Antibacterial Drug Design. *J Med Chem.* 2011; 54(4):915-929.
- L'heureux N, Paquet S, Labbé R, Germain L, Auger FA. A completely biological tissue-engineered human blood vessel. *FASEB J.* 1998; 12(1):47-56.
- Ikpa CCB and Maduka TOD. "Antimicrobial Properties of Methanol Extract of *Dacryodes edulis* Seed and Determination of Phytochemical Composition Using FTIR and GCMS." *Chem Afr.* 2020; 3(4):927-935.